

# A widely-tunable high-speed transmitter using an integrated SGDBR laser-Semiconductor Optical Amplifier and Mach-Zehnder modulator

Jonathon S. Barton, Erik J. Skogen, Milan. L. Mašanović, Steven P. DenBaars, and Larry A. Coldren, *Member, IEEE*

*Abstract*— The first integrated SGDBR laser-/Semiconductor Optical Amplifier-Mach-Zehnder modulator transmitter is presented. Devices have 3dB bandwidth ranging from 13-18GHz corresponding to electrodes lengths that range between 200-300um long. This corresponds to a  $V_{pi}$  of 4.8-6.2V

*Index Terms*— Tunable laser, RF modulation, Photonic Integrated circuits, high speed lasers, Chirp, Linearity, Optoelectronic device.

## INTRODUCTION

Tunable lasers are desirable for a number of applications such as in networks requiring dynamic provisioning, the replacement of Distributed Feedback (DFB) lasers in Wavelength Division Multiplexing (WDM) systems, in phased radar systems, or for optical switching, and routing[1]. Recently, single-wavelength DFBs have been integrated with Electro-Absorption Modulators (EAMs)[2] and Mach-Zehnder (MZ) interferometer-based modulators[3]. Widely-tunable Sampled-Grating DBR lasers(SGDBR) have also been integrated with various components over the last few years such as Semiconductor Optical Amplifiers (SOAs)[4], EAMs [5], Mach-Zehnder (MZ) modulators [6,7], and wavelength monitors. Historically, discrete  $\text{LiNbO}_3$  Mach-Zehnder modulators have been used in a hybrid integration scheme with DFB lasers to achieve high performance. However, monolithic integration leads to reduced costs in packaging, polarization independence, lower insertion losses, and advanced functionality in more complex photonic integrated circuits (PICs), despite potential problems of optical and electrical crosstalk. In this paper, we will examine a novel transmitter that utilizes a SGDBR tunable laser, SOA and Mach-Zehnder modulator – as shown in Fig 1.

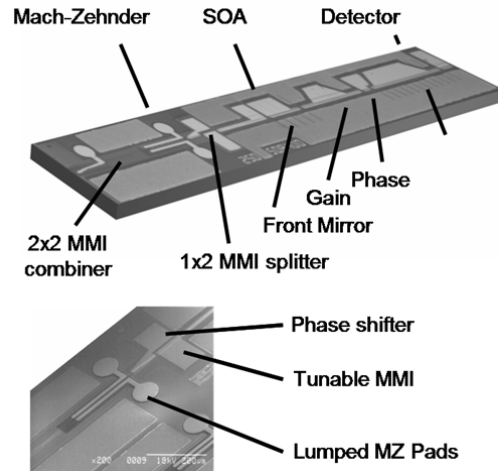


Fig. 1 MZ-SOA-SGDBR layout

In high bit-rate digital modulation systems ( $\geq 10\text{Gbit/s}$ ), chirp and fiber dispersion can limit the link's reach. Because of this, tailorable chirp modulators are preferable to generate both high-speed modulation and either negative or zero chirp depending on the application and the transmission fiber. Therefore, the aim of this work is to fabricate a compact monolithic transmitter that can simultaneously provide wide tunability, tailorable chirp, low insertion loss, superior power handling, low photocurrent generation, low drive voltage requirements, and high speed.

## DEVICE LAYOUT

The SGDBR laser consists of four sections: gain, phase, front mirror, and back mirror. The front and rear mirrors consist of periodically sampled DBR gratings to form a comb-like reflectivity spectrum [9]. The sampling periods in the front and back mirrors differ, which provides a different peak reflectivity spacing, so that only one set of mirror reflectivity peaks is aligned within the desired tuning range. By differentially tuning the front and back mirrors a small amount, adjacent reflectivity peaks can be

aligned, and the laser will operate at this new wavelength [9]. The SGDBRs use a 5 period front sampled-grating mirror with  $4\mu\text{m}$  wide bursts using a  $68.5\mu\text{m}$  period and a 12 period rear sampled-grating mirror with  $6\mu\text{m}$  wide bursts and  $61.5\mu\text{m}$  period. The tunable laser length is  $1.75\text{mm}$ , consisting of the gain section ( $550\mu\text{m}$ ), phase section ( $75\mu\text{m}$ ), front and rear mirrors, and rear absorber section ( $100\mu\text{m}$ ).

A backside absorber has been monolithically integrated for measurement of power, and to decrease the requirements of the backside anti-reflective coating. Reflections back into the laser are detrimental and require minimization. This can be accomplished by using a few approaches. Multi Mode Interference (MMI) component lengths are optimized to minimize reflections and tapered such that reflections are not coupled back into the laser cavity – mostly important in the ‘off’ state. Additionally, the waveguide is weakly guided, interfaces between active and passive sections are angled, and a broadband multi-layer anti-reflective (AR) coating is employed at the output. The waveguide is continuous throughout the structure avoiding index discontinuities that may be found at butt-coupled regrowth interfaces.

Due to the fact that the mirrors are lithographically defined and the laser does not require facet reflections to operate, integration with other components becomes fairly simple. Since the different fabrication steps in the SGDBR process are compatible with either SOAs, detectors, MZ modulators, and/or EA modulator sections, fabrication of an integrated device is not much more difficult than fabrication of a SGDBR itself.

In the interest of added output power, the devices use an inline  $400\mu\text{m}$  SOA integrated after the laser as shown in Fig. 2 that uses the same offset-quantum well active region as the gain section of the SGDBR.

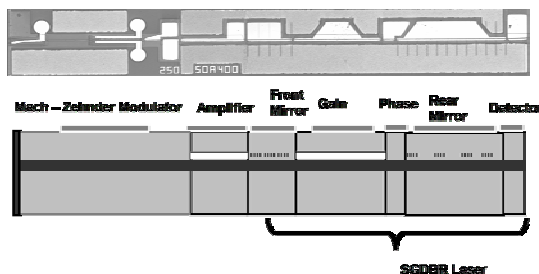


Fig. 2 Device epitaxial structure across the device. Offset QWs in SOA and Gain section.

### Passive waveguide in Mach-Zehnder, phase and mirror sections

The Mach-Zehnder interferometer is contacted with four electrodes. In order to facilitate push-pull high-speed RF modulation, symmetrical RF electrode pads with lengths of  $200\mu\text{m}$ ,  $250\mu\text{m}$  and  $300\mu\text{m}$  are explored. As the index can be changed due to current injection roughly a factor of 5 times greater in forward bias as in reverse bias, a separate  $100\mu\text{m}$  forward-biased DC phase tuning electrode is employed in one branch of the MZ structure. Finally there is a current injected MMI electrode for tuning the splitting ratio of power injected into the two branches.

Throughout the laser, the ridge waveguide is  $3\mu\text{m}$  wide. However, in the modulator section, the waveguides taper down to a  $2.5\mu\text{m}$  width for lower capacitance. Low-k Cyclotene 4024-40 (BCB) is photo-defined in regions only under the RF modulator pads. An additional electrode is placed on one of the curved outputs that can serve as a power tap or detector – which in reverse bias will reduce reflections.

The laser input uses a  $97\mu\text{m}$  long MMI with curved waveguides extending to a separation of  $20\mu\text{m}$  in between the two branches as shown in Fig. 3.

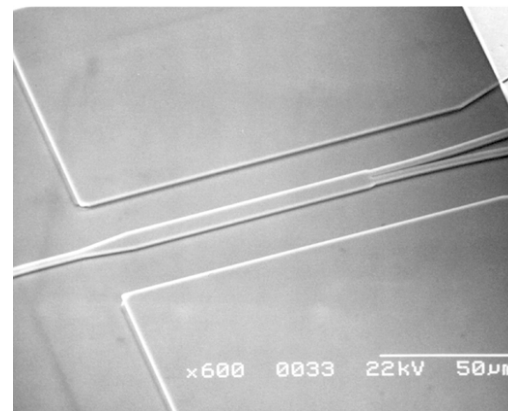


Fig. 3  $1 \times 2$   $97\mu\text{m}$  long multi-mode interference (MMI) splitter/combiner.

The output coupler is a  $2 \times 2$  MMI  $170\mu\text{m}$  long and  $10\mu\text{m}$  wide with two output waveguides curved at the facet for reduced reflections – so that the AR coating requirements are minimized. Fig. 4 shows this waveguiding structure and the regions in which  $\text{H}^+$  electrical isolation is performed.

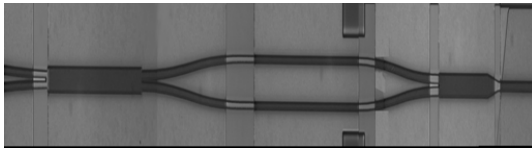


Fig. 4 Waveguiding structure of the Mach-Zehnder. Note the 1x2 input MMI and 2x2 output MMI.

The total device length is then 3.4mm, consisting of the 1.75mm SGDBR, 0.4mm SOA and 1mm MZ device with integrated curved waveguide passive regions at the facets. The MZ region epi-structure is passive and identical to that of the phase section in the laser with respect to doping and compositions as shown in Fig 2.

## PROCESS

The epitaxial layer structure, shown in Fig. 5, was grown on a sulfur-doped InP substrate using a Thomas Swan horizontal-flow rotating-disc MOCVD reactor.

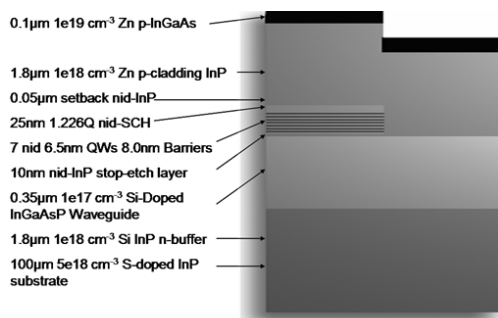


Fig. 5 Active/Passive offset-quantum well structure

First, the regions where gain is not required were made optically non-absorptive by the selective removal of the multiple quantum well stack (MQW) using a wet etch process – stopping on the 10nm non-intentionally doped InP stop-etch layer. Next, the sampled-grating mirrors were defined using holography in which single-order DBR gratings with a depth of 75nm were fabricated into the waveguide using a  $\text{Si}_3\text{N}_4$  sampling mask. A MOCVD regrowth was performed over the gratings providing the p-InP cladding and lattice-matched InGaAs contact layers. Following the regrowth, a surface ridge was RIE etched approximately  $1\mu\text{m}$  into the material and a subsequent 3:1  $\text{H}_3\text{PO}_4$ :HCl cleanup wet etch performed to define the ridge leaving a low scattering loss waveguiding

structure. Electrical isolation was provided by a schedule of proton implants in between laser, modulator, and SOA sections. The InGaAs layer was also selectively removed to aid electrical isolation. This procedure was intended to improve both current leakage in the laser and parasitic capacitance in the modulator sections. Top-side n-contacts were deposited using a Ni/AuGe/Ni/Au alloyed contact annealed at 430C. P-contacts used a Ti/Pt/Au layer structure. The substrates were lapped to a thickness of  $100\mu\text{m}$ , and a Ti/Pt/Au contact was deposited for the back-side n-contact and annealed at 410C. The devices were cleaved into bars and AR coated. The die were separated, soldered to aluminum nitride carriers, and wire bonded, for continuous-wave testing.

## DC MODULATOR CHARACTERISTICS

Typical extinction ratio curves for different lengths of Mach-Zehnder RF pads are shown in Fig. 6.

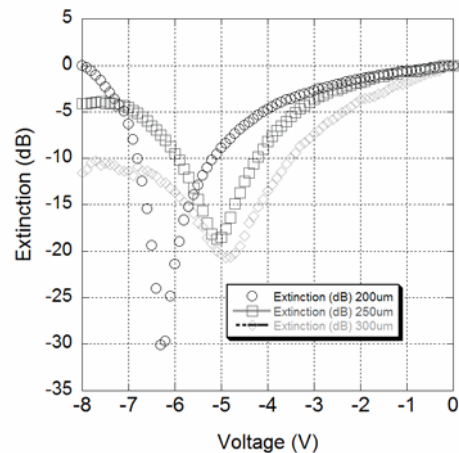


Fig. 6 Typical extinction response curves with different Mach-Zehnder RF electrode lengths at a wavelength of 1570nm

If the device is operated near the null or ‘off state’ one can achieve over 18dB of extinction with a low drive voltage. However, if operated far away from this null, only 5-6 dB change is possible. The forward-biased phase shifter can be used to provide the optimum phase shift to yield a low drive voltage for a given wavelength.

## RF RESULTS

A low k dielectric under the RF electrodes lowers the parasitic capacitance of the ridge structure considerably. The RF electrodes use a 300nm SiO<sub>2</sub> / 2.5μm BCB / 100nm SiO<sub>2</sub> sandwich of dielectric beneath the electrode pads as shown in Fig. 7.

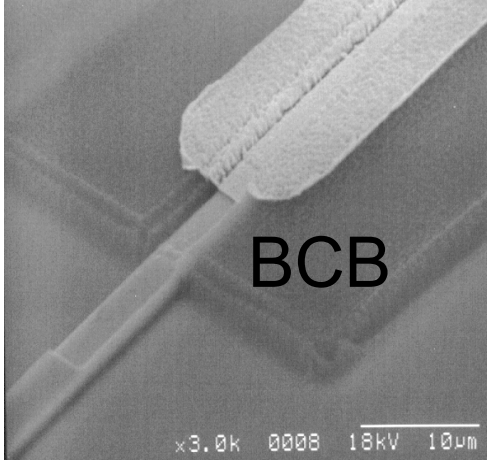


Fig. 7 SiO<sub>2</sub>/BCB/SiO<sub>2</sub> dielectric stack with RF electrode pad

This dielectric stack is then thicker than the height of the ridge itself – lending itself to reduced parasitic capacitance.

Figure 8 shows a comparison of the electrical/optical S<sub>21</sub> for different length MZ pads under single-sided modulation.

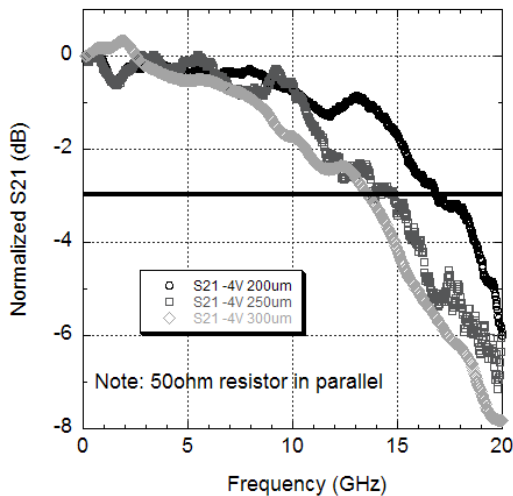


Fig. 8 3dB Bandwidth as a function of modulator length at V<sub>dcbias</sub> = -4V

The device is configured with a 50 ohm resistor in parallel. Each is shown for a bias of -4V. For each length as the depletion region is extended with reverse bias, the bandwidth is improved. This corresponds to a 3-4GHz change with bias from -1V to -4V. These devices should be suitable for 10Gbit/s modulation. For higher-speed applications, the design can be further refined with the use of traveling wave electrodes.

The low capacitance structure is due to not only the low parasitic capacitance of the BCB layer, but a large low n-doped region in the waveguide. Fig. 9 shows the Zn-doping profile in the passive section.

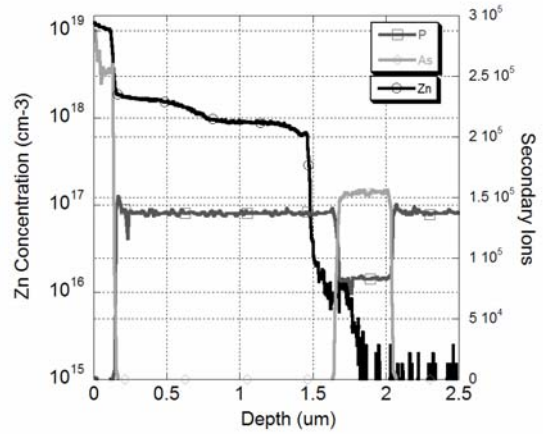


Fig. 9 Secondary Ion Mass spectroscopy (SIMS) of Zn in epitaxial layer structure

The step in the plot corresponds to InGaAsP waveguide. The Zn doping drops off approximately 0.2μm away from the waveguide giving a large depletion region and low free carrier losses in the waveguide.

As shown in fig. 10, small-signal chirp (linewidth enhancement factor) measurements were performed as a function of bias using both a single-sided RF electrode bias scheme, and a push-pull scheme using a RF hybrid coupler to achieve RF data and inverting data on the two 300μm electrode RF electrodes. The measurement was performed using a technique as described in[10] to determine the magnitude and sign of the chirp. Since the chirp parameter

is given as:  $\alpha = \frac{dn}{dk}$ , near the maximum or minimum in the output intensity, where the

intensity does not change much – there is still a significant phase change, and thus a large chirp parameter at this bias point. There is an inflection point in the chirp parameter at the peak of the ‘on’ state or the minimum in the ‘off’ state in which the chirp goes from strongly negative to strongly positive. For transmission experiments, it is the large-signal chirp parameter that is of most importance – particularly in the region of the 3dB ‘on’ state [14].

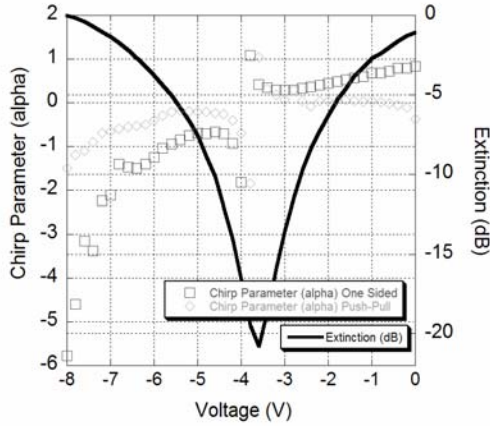


Fig. 10 Small-signal chirp parameter (linewidth enhancement factor) for both single side drive and push-pull drive and Optical extinction as a function of DC bias #1 at 1575.5nm. DC bias #2 = -4V. Phase shifter = 2.56mA for a pi phase shift shift at zero bias on both MZ branches.

We note that as expected, by using a push-pull bias scheme the chirp in each of the branches will cancel and the net chirp is improved as shown in fig 10 for a representative wavelength of 1575.5nm. Slight changes in bias can tailor the large-signal chirp parameter for the desired application – whether it is zero chirp or slightly negative chirp particularly interesting is higher bit rate applications ( $\geq 10\text{Gbit/s}$ ).

#### INTEGRATED SOA CHARACTERISTICS

The transmitters make use of an integrated SOA before the MZ modulator. This active section provides not only added gain, but helps to even out the wavelength dependent power variation as the gain is higher for lower optical input powers. Fig. 11 shows the gain characteristics as a function of current bias on the SOA for different lengths of devices.

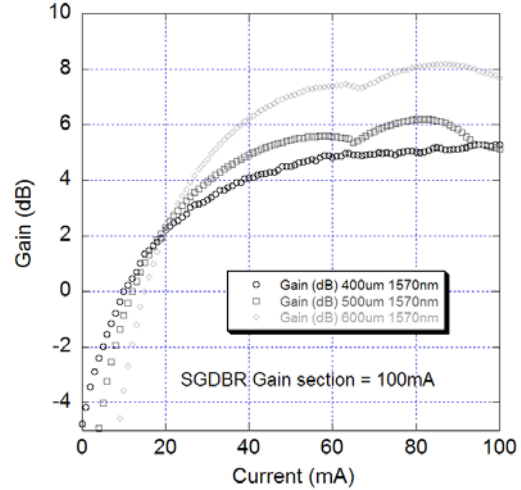


Fig. 11. SOA Gain as a function of SOA length

The output power of the SGDBR with 100mA corresponds to approximately 2mW into the SOA. Due to the flaring and angling of the output waveguide, we experience 5dB of coupling loss into a fiber. The transparency current of the 400 $\mu\text{m}$  is 12.4mA, 14.3mA for 500 $\mu\text{m}$  and 16.4mA for the 600 $\mu\text{m}$  SOA corresponding to a wavelength of 1570nm.

#### DISCUSSION

As these photonic integrated circuits (PICs) become more complex – with conflicting optimum layer structures, tradeoffs in design must be considered. A technique to establish different bandgaps across the wafer could be employed using for example either a butt-joint regrowth[12] of the modulator sections or quantum well intermixing(QWI) to fabricate low loss active-passive interfaces of varying compositions[11]. In order to achieve adequate tuning (6nm) the waveguide composition emission wavelength of 1.4 $\mu\text{m}$  (1.4Q) needs to be fairly close to the operating wavelength without increasing the on-state internal loss excessively. The modulator section becomes increasingly efficient as the composition approaches the operating wavelength as well due to higher order electro-optic effects. However, at these compositions, the device becomes more wavelength sensitive and subject to Franz-Keldysh electroabsorption in reverse bias. Regardless, for a relatively narrow wavelength range of 40-50nm, the  $V_{\text{pi}}$  changes only approximately 0.5V as a function of wavelength.

We believe that these results are very

encouraging in demonstrating a monolithically integrated widely-tunable transmitter with chirp tailorability. With additional optimization of the doping structure and waveguide composition, we expect the performance and efficiency to improve even further.

#### ACKNOWLEDGEMENTS

We thank DARPA-RFLICS for funding and Charles-Evans for providing the SIMs data.

#### REFERENCES

[1] Coldren LA. "Monolithic tunable diode lasers." *IEEE Journal of Selected Topics in Quantum Electronics*, vol.6, no.6, Nov.-Dec. 2000, pp.988-99. Publisher: IEEE, USA.

[2] Akage Y, Kawano K, Oku S, Iga R, Okamoto H, Miyamoto Y, Takeuchi H. "Wide bandwidth of over 50 GHz travelling-wave electrode electroabsorption modulator integrated DFB lasers." *Electronics Letters*, vol.37, no.5, 1 March 2001, pp.299-300. Publisher: IEE, UK.

[3] Xun Li, Huang W-P, Adams DM, Rolland C, Makino T. "Modeling and design of a DFB laser integrated with a Mach-Zehnder modulator." *IEEE Journal of Quantum Electronics*, vol.34, no.10, Oct. 1998, pp.1807-15. Publisher: IEEE, USA.

[4] Mason B, **Barton J**, Fish GA, Coldren LA, Denbaars SP. "Design of sampled grating DBR lasers with integrated semiconductor optical amplifiers." *IEEE Photonics Technology Letters*, vol.12, no.7, July 2000, pp.762-4. Publisher: IEEE, USA.

[5] Mason B, Fish GA, DenBaars SP, Coldren LA. "Widely tunable sampled grating DBR laser with integrated electroabsorption modulator." *IEEE Photonics Technology Letters*, vol.11, no.6, June 1999, pp.638-40. Publisher: IEEE, USA.

[6] Barton JS., Skogen, E.J. , Masanovic M., S. Denbaars, L. A. Coldren, "Integration of a Mach-Zehnder Modulator with Sampled Grating Distributed Bragg Reflector Laser," *Proc. Integrated Photonics Research Conference*,

*paper no. 1FC3-1, Vancouver, Canada, July 17-19 2002.*

[7] Barton JS, Skogen EJ, Masanovic ML, DenBaars SP, Coldren LA. "Tailorable chirp using integrated Mach-Zehnder modulators with tunable sampled grating distributed Bragg reflector lasers." *2002 IEEE 18th International Semiconductor Laser Conference. Conference Digest (Cat. No.02CH37390). paper no. TuB3, Garmisch, Germany (Sept. 29- Oct. 3) IEEE. 2002, pp.49-50. Piscataway, NJ, USA.*

[8] Fish GA. "Monolithic widely-tunable DBR lasers." *OFC 2001. Optical Fiber Communication Conference and Exhibit. Technical Digest Postconference Edition (IEEE Cat. 01CH37171). Opt. Soc. America. Part vol.2, 2001, pp.TuB1 no. 1-4 Washington, DC, USA.*

[9] Jayaraman V, Chuang Z-M, Coldren LA. "Theory, design, and performance of extended tuning range semiconductor lasers with sampled gratings." *IEEE Journal of Quantum Electronics*, vol.29, no.6, June 1993, pp.1824-34. USA

[10] Devaux F, Sorel Y, Kerdiles JF. "Simple measurement of fiber dispersion and of chirp parameter of intensity modulated light emitter." *Journal of Lightwave Technology*, vol.11, no.12, Dec. 1993, pp.1937-40. USA.

[11] Skogen EJ, Barton JS, Denbaars SP, Coldren LA. "A quantum-well-intermixing process for wavelength-agile photonic integrated circuits." *IEEE Journal of Selected Topics in Quantum Electronics*, vol.8, no.4, July-Aug. 2002, pp.863-9. Publisher: IEEE, USA.

[12] Binsma JJM, Thijs PJA, Van Dongen T, Jansen EJ, Staring AAM, Van den Hoven GN, Tiemeijer LF. "Characterization of butt-joint InGaAsP waveguides and their application to 1310 nm DBR-type MQW gain-clamped semiconductor optical amplifiers." *IEICE Transactions on Electronics*, vol.E80-C, no.5, May 1997, pp.675-81. Publisher: Inst. Electron. Inf. & Commun. Eng, Japan.

[13] Aoki M, Suzuki M, Sano H, Kawano T, Ido T, Taniwatari T, Uomi K, Takai A. "InGaAs/InGaAsP MQW electroabsorption modulator integrated with a DFB laser fabricated by band-gap energy control selective area MOCVD." *IEEE Journal of Quantum*

Electronics, vol.29, no.6, June 1993, pp.2088-96. USA.

[14] Dorgeuille F., Devaux F., "On the Transmission Performances and the Chirp Parameter of a Multiple-Quantum-Well Electroabsorption Modulator." IEEE Journal of Quantum Electronics, vol. 30., no. 11, Nov. 1994, pp. 2565-2572. USA.

### Author Biographies

**Jonathon S. Barton** was born in Sacramento, California in 1975. He received his bachelor's degree in Electrical Engineering and Material Science in 1998 from the University of California, Davis. He currently is a Ph.D student in Larry Coldren's group at the University of California Santa Barbara. His research interests focus on photonic integrated circuits – integrating tunable lasers with semiconductor optical amplifiers and modulators.

**Erik J. Skogen** was born in Minneapolis, Minnesota in 1975. He received the B.S. degree from Iowa State University in 1997, and the M.S. degree from the University of California, Santa Barbara in 1999. He is currently pursuing the Ph.D. degree in electrical and computer engineering from the University of California, Santa Barbara. His current research interests include, widely-tunable semiconductor lasers, monolithic integration for photonic integrated circuits, growth aspects in the InGaAsP material system using MOCVD, and quantum well intermixing.

**Milan Mašanović** graduated from the School of Electrical Engineering, University of Belgrade, Serbia in 1998. He received his M.S. degree from the Department of Electrical and Computer Engineering, University of California Santa Barbara in 2000, where he is currently pursuing his Ph.D. His research interests include novel photonic integrated circuits in indium phosphide, wavelength conversion and optical label swapping.

**Steven P. Denbaars** Dr. Steven P. DenBaars is an Associate Professor of Materials and Electrical Engineering at the University of California Santa Barbara. He received his PhD. degree in Electrical Engineering from the University of Southern California, in 1988 under the direction of Prof. P.D. Dapkus. From 1988-1991 Prof. DenBaars was a member of the technical staff at Hewlett-Packard's Opoelectroncis Division involved in the growth and fabrication of visible LEDs. His current research interests are in metalorganic chemical vapor deposition (MOCVD) of III-V compound semiconductor materials and devices. Specific research interests include growth of wide-bandgap semiconductors (GaN based), and their application to Blue LEDs and lasers and high power electronic devices. This research has lead to the first US university demonstration of a Blue GaN laser diode and over 7 patents pending on GaN growth and processing. He is the lead investigator of the ARPA funded Multi-univerisity Nitride Consortium which will develop and transfer GaN technology to industry. In 1994 he received a NSF Young Investigator award. He has Authored or Co-Authored over 130 technical publications, 100 conference presentation, and 10 patents.

**Larry Coldren** Prior to coming to UCSB in 1984, Professor Coldren worked on guided surface-acoustic-wave devices, microfabrication techniques, and tunable diode lasers at AT&T Bell Laboratories. At UCSB he has worked on a variety of optoelectronic materials and devices currently focusing on components and fabrication techniques for III-V optoelectronic integrated circuits. His group has made seminal contributions to vertical-cavity lasers and widely-tunable lasers, and they are now involved in optical switching and noiseless amplification research. The fundamentals of such components are detailed in his recent book entitled Diode Lasers and Photonic Integrated Circuits,

published by Wiley. Professor Coldren is also heavily involved in new materials growth and fabrication technology essential to the fabrication of such integrated optoelectronic components. Most recently, his group has become

actively involved in the fabrication of GaN-based edge- and vertical-cavity lasers that will emit in the blue and green. Professor Coldren has been a Fellow of [IEEE](#) since 1982 and a Fellow of [OSA](#) since 1990.